ACS APPLIED MATERIALS & INTERFACES

Research Article

www.acsami.org

Stable Organic–Inorganic Hybrid of Polyaniline/α-Zirconium Phosphate for Efficient Removal of Organic Pollutants in Water Environment

Lei Wang,[†,‡,∥] Xi-Lin Wu,[†,§,∥] Wei-Hong Xu,*[,†,‡] Xing-Jiu Huang,[‡] Jin-Huai Liu,[‡] and An-Wu Xu*[,†]

[†]Department of Chemistry, Division of Nanomaterials and Chemistry and [§]College of Nuclear Science and Technology, University of Science and Technology of China, Hefei, Anhui 230026, PR China

[‡]Research Center for Biomimetic Functional Materials and Sensing Devices, Hefei Institute of Intelligent Machines, Chinese Academy of Sciences, Hefei, Anhui 230031, PR China

Supporting Information

ABSTRACT: In this article, organic–inorganic hybrid materials of polyaniline/α-zirconium phosphate (PANI/α-ZrP) was synthesized by in situ oxidative polymerization reaction and characterized by Fourier transformed infrared (FTIR), field-emission scanning electron microscopic (FE-SEM) and X-ray diffraction (XRD). The results showed that polyaniline (PANI) was successfully grown on the surface of α-zirconium phosphate (α-ZrP) nanoplates. The PANI/α-ZrP nanocomposites were further applied to remove methyl orange (MO), which was used as a model of organic pollutants in aqueous solution. A synergistic effect of PANI and α-ZrP on promoting the adsorption removal of MO was observed. The PANI/α-ZrP nanocomposites exhibited excellent maximum adsorption capacity toward MO (377.46 mg g^{-1}), which is superior to that of PANI nanotubes (254.15 mg g^{-1}) and much higher than that of many other adsorbents. The adsorption isotherms of MO can be well-fitted with the Langmuir model and the adsorption kinetics follows the pseudo-second-order model. MO adsorption decreased with increasing solution pH at pH > 4.0 implying that MO adsorption on PANI/α-ZrP may via electrostatic interactions between amine and imine groups on the surface of PANI/α-ZrP and MO molecules. This study implies that the hybrid materials of PANI/α-ZrP can be suggested as potential adsorbents to remove organic dyes from large volumes of aqueous solutions.

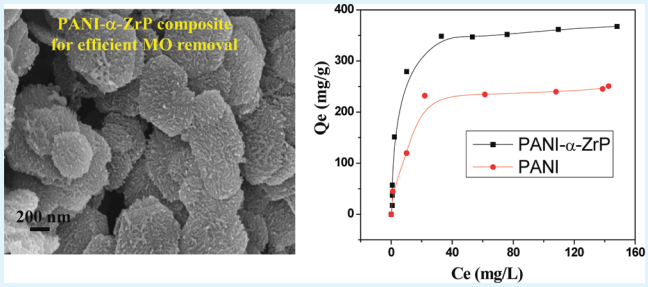

KEYWORDS: *polyaniline/α-zirconium phosphate, nanocomposites, methyl orange, adsorption*

1. INTRODUCTION

Many textile and printing industries that use dyes and pigments release a large amount of highly colored effluent in their wastewater. The used dyes may cause an eco-toxic hazard and induce the potential danger of bioaccumulation.[1] Various techniques including biological treatment, adsorption, chemical oxidation, coagulation, membrane filtration, and photochemical degradation have been used to remove dyes from colored wastewater.[2] Among these techniques, adsorption is considered as one of the best available technologies due to its effectiveness, operational simplicity, low cost and low energy requirements. Several adsorbents have been reported for removal of organic dyes such as clay,[3,4] rice husk,[5] activated carbon,[6] red mud,[7] and fly ash.[8,9] Activated carbon is one of the most widely used adsorbents but it has some drawbacks such as costly regeneration, high attrition rate and poor selectivity.[10] Other materials like clay, rice husk, red mud, and fly ash are readily available but of poor effectiveness. Thus, many present studies focused their efforts on developing novel alternative adsorbents with high adsorptive capacity and low cost.

Recently, studies of organic–inorganic hybrid materials for adsorbents applications have attracted a wide range of interests because of their enhanced adsorption and multifunctional properties. For example, Paul et al. reported that organic–inorganic hybrid microporous organosilica shows very high adsorption capacity toward metal ions like Fe^{3+}, Cu^{2+}, and Zn^{2+}.[11] Swain et al. found that zironium(IV)/propanolamine composites have good efficiency for removal of fluoride from drinking water.[12] Jin et al. fabricated poly(acrylic acid-acrylonitrile)/attapulgite composite and found that it holds a good adsorption selectivity to Pb^{2+} among numerous metal ions and high adsorption capacity toward phenol.[13] Wang et al. found that polyacrylonitrile/ferrous chloride composite porous nanofibers have excellent adsorption capacity toward $Cr_2O_7^{2-}$ anion.[14] Very recently, the use of nanomaterials as adsorbents has received much attention because of the unique structural and surface properties of them.[15] However, the study of

Received: February 24, 2012
Accepted: April 30, 2012
Published: April 30, 2012

 © 2012 American Chemical Society

nanomaterial-based organic−inorganic composites for water treatment is still in the early stage.

α-ZrP is a cationic layered compound, which is mainly used as ion-exchanger, catalyst, sorbent and so on.[16] Polyaniline (PANI) is a common polymer that has many specific properties such as high capacitive characteristics, low cost, ease of synthesis, good environmental stability and adjustable electrical conductivity.[17−19] The presence of amino and imine groups on PANI may provide possible adsorption sites for biding organic and inorganic molecules. Incorporating the organic PANI to the inorganic α-ZrP to obtain the organic−inorganic hybrid materials of PANI/α-ZrP may preserve or even improve the major features of each phase in the hybrid materials, and furthermore, new properties may come from the synergy of both components.[20] Thus, utilizing a strategy to prepare organic−inorganic hybrid material of PANI/α-ZrP for water treatment would be of significance.

In this study, organic−inorganic hybrid material of PANI/α-ZrP nanocomposites were synthesized by in situ oxidative polymerization reaction. The aim of this work is to investigate the possibility of using the PANI/α-ZrP nanocomposites for the adsorptive removal of organic pollutants. Methyl orange (MO) serves as a model compound of the harmful and water-soluble organic pollutants, which are widely used in textile industries and harmful to the environment. The adsorption properties of MO on PANI/α-ZrP were studied by batch experiment. The kinetics and isotherm models were applied to study the adsorption mechanism. To the best of our knowledge, this is the first example of using stable PANI/α-ZrP organic−inorganic nanocomposites for efficient removal of MO from aqueous solution. The PANI/α-ZrP nanocomposites can be suggested as a suitable material for the efficient removal of organic pollutants from aqueous solution.

2. EXPERIMENTAL SECTION

Chemicals. Zirconyl chloride octahydrate ($ZrOCl_2·8H_2O$, 98%) and phosphoric acid (85%) were purchased from Sigma-Aldrich Co. (USA). Aniline, ammonium persulfate (APS), tartaric acid, methyl orange (MO), methylene blue (MB) and Congo red (CR) were purchased from Sinopharm Chemical Reagent Co., Ltd. (China). All above reagents were used as received. Milli-Q ultrapure water (18.2 MΩ·cm) was used for all the experiments.

Characterization. The morphologies of PANI/α-ZrP were observed by a field-emission scanning electron microscope (FE-SEM, Sirion 200). X-ray diffraction (XRD) patterns were recorded in the range of 2θ = 5−65° with a Philips X'Pert X-ray diffractometer. Infrared spectra were recorded on a JASCO FTIR 410 spectrophotometer with the KBr pellet technology. The Barrett-Emmett-Teller (BET) specific surface of PANI/α-ZrP was measured by a Micromeritics ASAP 2010 system at 77 K by the N_2 adsorption−desorption. The UV−vis spectrum was carried out on a UV-3000 spectrophotometer. The zeta-potential was measured by a ZETASIZER 3000 HSA system.

Sample Preparation. The α-zirconium phosphate nanoplates were prepared following the synthetic process described in an earlier report.[21] Briefly, 3.0 g of $ZrOCl_2·8H_2O$ was mixed with 30.0 mL of H_3PO_4 (6.0 M) in a sealed Teflon-lined pressure vessel and reacted at 200 °C for 24 h. After the reaction, the product was washed and collected by centrifugation for three times. Then, the solid was then dried at 65 °C for 24 h. The dried α-ZrP was ground with a mortar and pestled into fine powders.

PANI/α-ZrP nanocomposites were prepared by in situ oxidative polymerization reaction. First, 0.1 g of α-ZrP was dispersed in a 50:50 mixture of H_2O and ethanol (50 mL) and the mixture was ultrasonicated for about 10 min to obtain well-dispersed colloidal suspensions. A desired amount of aniline (the mol ratio α-ZrP/aniline = 1:30) dissolved in ethanol was added dropwise to the above α-ZrP colloidal suspensions under constant stirring at 750 rpm. These mixtures were then stirred at room temperature for 24 h. Then the pH of the solution was adjusted to 3.0 by adding definite amount of tartaric acid. After that, the mixture was cooled in an ice−water bath, subsequently by adding 10 mL of oxidant aqueous solution containing definite amount of APS precooled in the ice−water bath for 5 min. The polymerization reaction was carried out in the ice−water bath under constant stirring. Finally, the dark green PANI/α-ZrP product was obtained and the solid was centrifugated, washed with deionized water and ethanol several times and dried in an oven at 60 °C. As comparison, PANI/α-ZrP nanocomposites with α-ZrP/aniline mol ratio = 1:5, 1:10, 1:15, 1:20, and 1:40 were prepared by the same in situ oxidative polymerization reaction. PANI nanotubes were also prepared by a similar route in the absence of α-ZrP.

Adsorption Experiments. All the adsorption experiments were carried out in glass vials by using a batch technique. Before adsorption experiments, a calibration curve was obtained from the UV−vis spectra of the standard MO solutions (5−50 mg L^{-1}) at pH 4.0 (see the Supporting Information, Figure S1). For the kinetic experiments, an amount of 5 mg PANI/α-ZrP was ultrasonically dispersed into 20 mL of 100 mg L^{-1} MO solution for 1 min, and then the mixture was shaken for 24 h. Samples were withdrawn at appropriate time intervals and supernatant liquid was separated by centrifuging at 10 000 rpm for 3 min. For the adsorption isotherm experiments, an amount of 5 mg of PANI/α-ZrP was added to 20 mL of a MO solution (various concentrations). After the suspensions were oscillated for 24 h, the solid and liquid phases were separated by centrifugation at 10 000 rpm for 5 min. Then the concentration of MO in the supernatant liquid was determined by UV−vis absorption spectroscopy. The adsorbed amounts of MO were calculated by using the following equation

$$q_e = \frac{(C_0 - C_e)V}{m} \quad (1)$$

where C_0 and C_e are the initial and equilibrium concentrations of MO (mg L^{-1}) respectively, V is the volume of solution (L) and m is the mass of PANI/α-ZrP used (g). For the effect of pH, an amount of 5 mg of PANI/α-ZrP was ultrasonically dispersed into 20 mL of 80 mg L^{-1} MO solution and the pH of the solution was adjusted by NaOH and HCl with a pH meter.

3. RESULTS AND DISCUSSION

Characterization. The XRD patterns of α-ZrP nanoplates and PANI/α-ZrP nanocomposites are shown in Figure 1. The typical diffraction peaks at 2θ = 11.6, 19.8, 25.0, 34.13, and 37.33° correspond to the primary diffraction of the (002), (110), (112), ($\bar{2}06$), and ($\bar{1}16$) planes of the α-ZrP, respectively.[21] The interlayer distance of (002) plane was estimated from Bragg's law, and the d-spacing is 7.6 Å, in agreement with previous reports.[21,22] The main characteristic

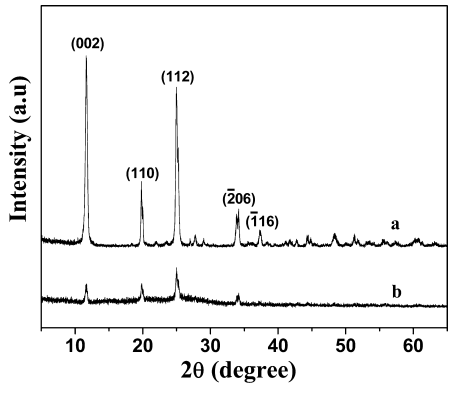

Figure 1. X-ray diffraction patterns of (a) α-ZrP and (b) PANI/α-ZrP.

peaks of the PANI/α-ZrP nanocomposites were almost the same with that of α-ZrP, which indicated that the crystal structure of PANI/α-ZrP was well-maintained after the grafting process under polymerization reaction.[23] The diffraction peaks for the PANI were not observed, demonstrating the relative thin layer and amorphous feature of the PANI synthesized by this in situ polymerization reaction.[23] The FTIR spectra of α-ZrP and PANI/α-ZrP are shown in Figure 2. The peaks at 1620

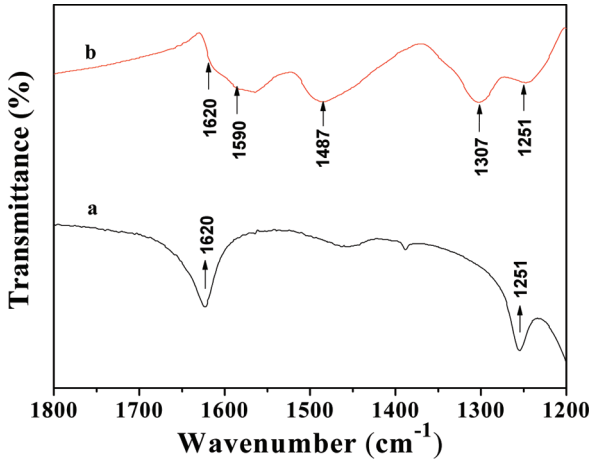

Figure 2. FTIR spectra of (a) α-ZrP and (b) PANI/α-ZrP.

and 1251 cm^{-1} are attributed to the water bending vibrations and P−OH stretching or deformation vibrations, respectively.[22,24] These are the characteristic peaks of α-ZrP, which also present in the FT-IR spectra of PANI/α-ZrP. The bands at 1590, 1487, and 1307 cm^{-1} are attributed to the C−C ring stretching and C−H bending or C−N stretching vibrations of PANI, implying the presence of PANI in the composites.[24,25]

FE-SEM images showed the size and shape of α-ZrP nanoplates, PANI nanotubes and PANI/α-ZrP nanocomposites. From Figure 3a, α-ZrP exhibits a uniform platelike hexagonal morphology, with a lateral dimension of approximately 300−600 nm and a thickness of about 20 nm. Figure 3b shows the as-synthesized PANI nanotubes with an average diameter of about 200 nm and very rough surface. Figure 3c and 3d show clearly that the platelike α-ZrP structures were encapsulated by PANI thin layer with uniform fibrillar nanostructure. As compared to PANI nanotubes synthesized in the absence of α-ZrP, it can be clearly seen that much smaller and uniformly dispersed PANI fibrillar nanostructure were grown on the α-ZrP surface, which could provide more active binding sites for MO. The BET surface area of PANI/α-ZrP nanocomposites was 30.40 $m^2 g^{-1}$.

Effect of Solution pH on Adsorption. The pH dependent adsorption of Methyl orange (MO) on PANI/α-ZrP nanocomposites is shown in Figure 4a. As the increase of solution pH, the adsorption of MO increased at pH < 4.0, while the adsorption gradually declined at pH >4.0. The PANI/α-ZrP nanocomposites showed the maximum adsorption capacity toward MO at pH 4.0. Thus, the kinetic and isotherm experiments were carried out at pH 4.0 in this study. To further understand the influence of pH on the MO removal process, we measured the values of zeta-potential of the PANI/α-ZrP nanocomposites at different pH and show them in Figure 4b. As can be seen, the electrostatic point of PANI/α-ZrP was about 6.0, indicating that at pH below 6.0 the PANI/α-ZrP nanocomposites are carrying positive charges due to the protonation of the imine and amine groups. MO molecules have the negative charges because of the anionic sulfonate groups. So the strong electrostatic forces between the protonated adsorbent and negatively charged MO anions occurred at low pH value, leading to the enhanced MO adsorption. However, at pH above 6.0, PANI/α-ZrP was

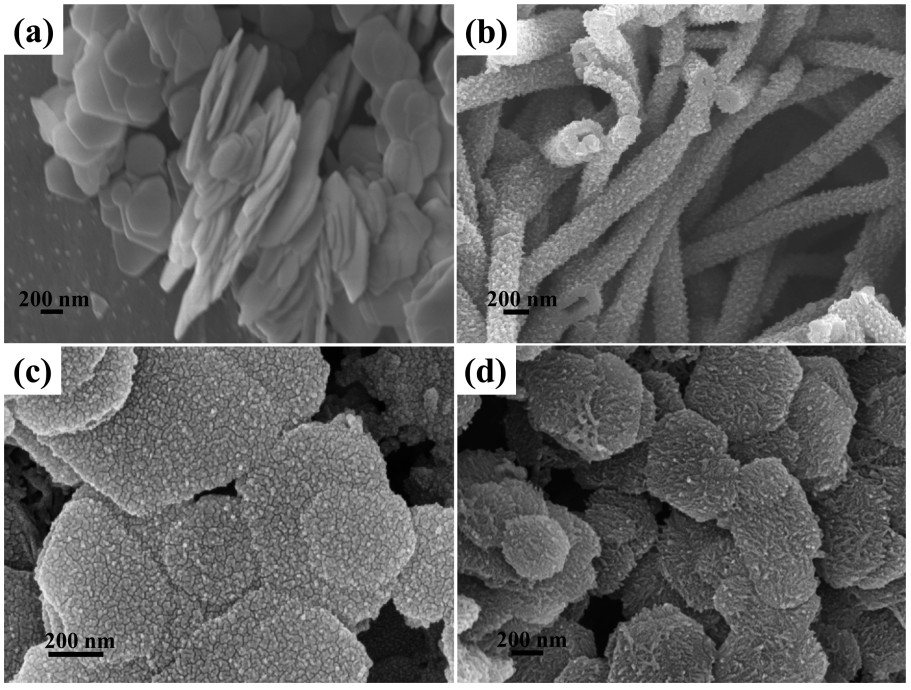

Figure 3. SEM images of (a) α-ZrP, (b) PANI, (c) PANI/α-ZrP (α-ZrP/aniline mol ratio = 1:20), and (d) PANI/α-ZrP (α-ZrP/aniline mol ratio = 1:30), respectively.

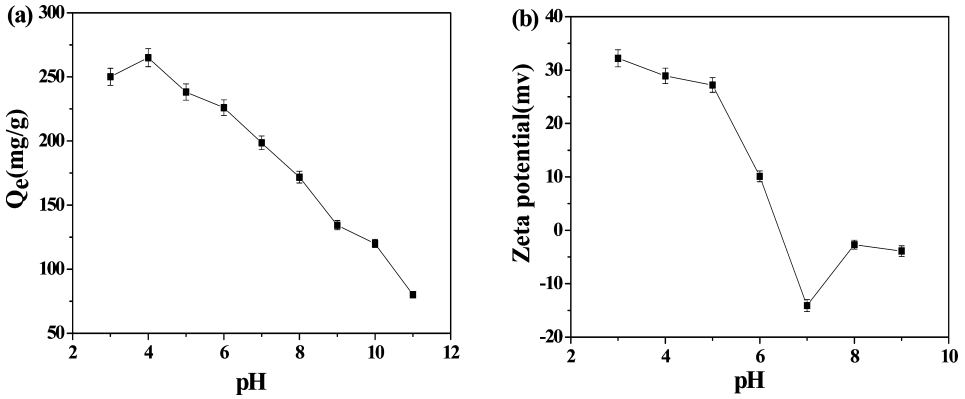

Figure 4. (a) Effect of pH on the removal of MO by PANI/α-ZrP nanocomposites and (b) Zeta-potential of PANI/α-ZrP nanocomposites as a function of pH.

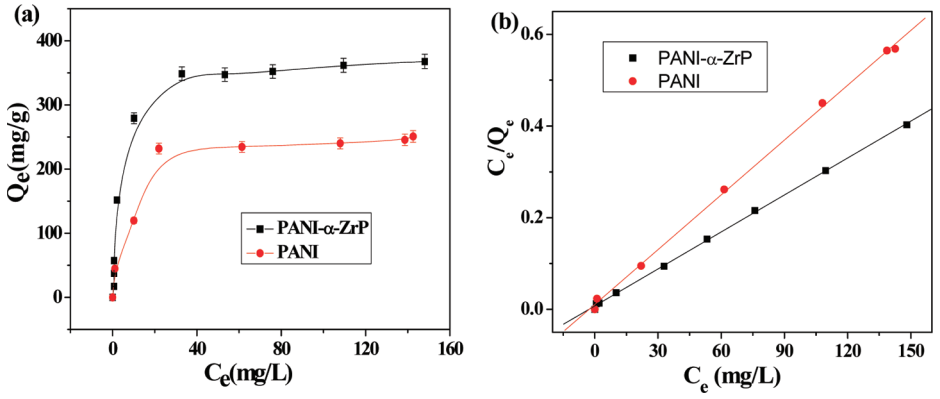

Figure 5. (a) Adsorption isotherms of MO on PANI nanotubes and PANI/α-ZrP nanocomposites and (b) Langmuir isotherm models for MO on PANI nanotubes and PANI/α-ZrP nanocomposites.

negatively charged because of the competitive adsorption of hydroxyl on imine and amine groups. Increasing pH might result in increased electrostatic repulsive force, leading to low adsorption of MO on PANI/α-ZrP. Further experiments of Congo red (CR) and methylene blue (MB) adsorption on PANI/α-ZrP nanocomposites as the function of pH were also carried out to testify the above mechanism. As can be seen in Figure S6 in the Supporting Information, under pH <4, the adsorption of CR is first increased as an increase in pH, while the adsorption of CR decreases slowly with pH increasing from 4.0 to 11.0. The adsorption behavior of CR on PANI/α-ZrP nanocomposites as the function of pH is consistent with that of MO, because both CR and MO are anionic dyes. However, the adsorption percentage of MB is gradually increased when the solution pH increases from 3 to 11. The different adsorption behaviors of CR and MB on sample are due to the fact that they carry opposite charges. These results further verify the pH effect on the adsorption properties and the electrostatic forces between the adsorbent and the dyes, which play an important role in the adsorption process.

Adsorption Isotherm. The adsorption isotherms are important data to understand the adsorption mechanism. Adsorption isotherms of MO onto PANI nanotubes and PANI/α-ZrP at 25 °C are shown in Figure 5a. It should be noted that the pure α-ZrP almost does not adsorb MO at all the pH range (see the Supporting Information, Figure S2). As can be seen in Figure S3 in the Supporting Information, the PANI/α-ZrP nanocomposites synthesized with α-ZrP/aniline mol ratio = 1:30 has the highest adsorption capacity toward MO. Thus, all the adsorption experiments were carried out by using this molar ratio. As shown in Figure 5a, the adsorption capacity of MO on PANI/α-ZrP is much higher than that of MO on PANI nanotubes, indicating that the nanostructures of PANI on the surface of α-ZrP might play an important role in MO adsorption. The binding sites of PANI/α-ZrP for MO mainly exist on the surface of PANI/α-ZrP. To further study the adsorption mechanism, Langmuir and Freundlich isotherm equations were used to fit the experimental data. The Langmuir[26] and Freundlich[27] isotherm models are applied to simulate MO adsorption on PANI nanotubes and PANI/α-ZrP nanocomposites. The Langmuir model is expressed as

$$\frac{C_e}{Q_e} = \frac{1}{q_m k_L} + \frac{C_e}{q_m} \quad (2)$$

The Freundlich isotherm model can be expressed by the following formula

$$Q_e = kC_e^{1/n} \quad (3)$$

where C_e is the equilibrium concentration of MO in the supernatant (mg L^{-1}); q_m represents the maximum adsorption capacity of MO on per weight of adsorbent (mg g^{-1}); k_L is the Langmuir constant related to the energy of adsorption (L mg^{-1}) and Q_e is the amount of MO adsorbed on per weight of adsorbent after equilibrium (mg g^{-1}); The Freundlich constant k is correlated to the relative adsorption capacity of the adsorbent (mg g^{-1}), and $1/n$ is the adsorption intensity. The fitting parameters for MO adsorption isotherms based on the

dx.doi.org/10.1021/am300335e | ACS Appl. Mater. Interfaces 2012, 4, 2686−2692

Langmuir and Freundlich isotherm equations are listed in Table 1. The Langmuir isotherm model fitted experimental data are shown in Figure 5b. The Freundlich isotherm model fitted experimental data can be seen in the Supporting Information, Figure S4. The fitting results showed that the relative coefficient (R^2) of the Langmuir model was higher than that of the Freundlich model, indicating that the adsorption of MO on PANI nanotubes and PANI/α-ZrP nanocomposites both follow the Langmuir isotherm model but not the Freundlich model. The fact that the sorption data of MO fitted with the Langmuir isotherm indicates that the adsorption of MO on these materials is a monolayer adsorption and the binding energy on the whole surface of PANI/α-ZrP nanocomposites is uniform.[28] On the basis of the Langmuir equation, the values of q_m are 254.15 and 377.46 mg g^{-1} for PANI nanotubes and PANI/α-ZrP nanocomposites, respectively. These values are quite in agreement with the experimental data shown in Figure 5a. The results demonstrate that the as-synthesized PANI/α-ZrP nanocomposites have a superior adsorption capacity toward MO. The superior adsorption capacity is due to the thin layer of PANI fibrillar nanostructures formed on the α-ZrP hexagonal nanoplates, which provide more active sites (amine and imine of nitrogen) for MO adsorption. For comparison, the maximum adsorption capacity of MO on PANI, PANI/α-ZrP nanocomposites and other adsorbents is listed in Table 2. It can be seen that the hybrid material of PANI/α-ZrP has the highest adsorption capacity toward MO as compared to the other adsorbents.[6,30−36] The nanostructure of the hybrid material with thin layer of fibrillar PANI is responsible for the ultra high adsorption capacity. In addition, the adsorption capacities of CR and MB on PANI/α-ZrP nanocomposites were also investigated (see the Supporting Information, Figure S7). The maximum adsorption capacities calculated by the Langmuir equations are 500 mg g^{-1} for CR and 156.25 mg g^{-1} for MB, respectively. PANI can be easily discharged into neutral salt in basic solution.[29] Thus, 0.5 M KOH was used for the desorption study. It was found that more than 90% MO can be desorbed from the PANI/α-ZrP composites by using 0.5 M KOH. For recycle study, about 80% of MO removal was retained after 5 cycles of reuse. The superior adsorption capacities and easily recyclable and reusable properties indicate that the PANI/α-ZrP nanocomposites could be a potential candidate for large volume wastewater treatment in the textile/printing industry. It could be further extended to treat other kinds of organic pollutants using this adsorbent in future practical applications.

Table 1. Summary of the Langmuir, and Freundlich Isotherm Model Parameters for the Adsorption of MO on PANI nanotubes and PANI/α-ZrP Nanocomposites

		Langmuir model parameters			Freundlich model parameters		
adsorbent	q_{exp} (mg/g)	k_1 (L·mg -1)	q_m (mg/g)	R^2	n	k	R^2
PANI/α-ZrP	370	0.36	377	0.999	2.18	53.3	0.82
PANI	250	0.037	254	0.999	2.95	53.2	0.89

Table 2. Comparison of the Maximum Absorption Capacity of MO on PANI/α-ZrP Nanocomposites with Other Different Adsorbents

adsorbents	adsorption capacity (mg g^{-1})	pH	ref
modified sporopollenin	5.23		30
activated carbon	9.49	4.0	6
orange peels	20.50	5.7	31
banana peels	21	5.7	31
hyper-cross-linked polymer	70.92		32
Zn/Al-LDO	181.90	6.0	33
lapindo volcanic mud	333.30	3.0	34
NH_3^+-MCM-41	366.57	5.6	35
polyaniline microspheres	154.56		36
polyaniline nanotubes	254.15	4.0	our work
polyaniline/α-ZrP	377.46	4.0	our work

Adsorption Kinetics. The adsorption kinetics are used to evaluate the adsorption characteristics of MO on the PANI nanotubes and PANI/α-ZrP nanocomposites. As can be seen in Figure 6a, the adsorption amount increased rapidly in the initial stage in first 60 min, and then slowed down until the sorption process reached equilibrium. The beginning rapid step of MO sorption is due to the surface physical sorption because of the existence of a large number of sorption sites (amine and imine of nitrogen) on the surface of PANI nanotubes and PANI/α-ZrP nanocomposites. The subsequent slow step is attributable to the limited active adsorption sites available on the surface of the adsorbents, and the MO adsorbed on the surface would further hamper the diffusion of other MO, resulting in a rather long time to reach the equilibrium.[12] It is also observed from Figure 6a that the amount of MO adsorbed by PANI/α-ZrP nanocomposites is larger than that adsorbed by PANI nanotubes, which is consistent with the results of the adsorption isotherms (Figure 4a). The pseudo-first-order model and pseudosecond-order model were used to simulate the kinetics adsorption of MO onto both the PANI nanotubes and PANI/α-ZrP nanocomposites (Figure 6b). The pseudo-second-order kinetic model can be expressed by the following equation[37]

$$\frac{t}{Q_t} = \frac{1}{k_2 Q_e^2} + \frac{t}{Q_e} \quad (4)$$

where Q_e and Q_t are the amounts of MO adsorbed on the adsorbents (mg g^{-1}) at equilibrium and at time t (min), respectively, and k_2 is the rate constant (g·mg^{-1}·min). As can be seen in Figure 6b, the plots of t/Q_t versus t is linear for the two kinds of materials (correlation coefficient R^2 = 0.999 and 0.999 for PANI/α-ZrP and PANI nanotubes, respectively). As compared with the pseudo-first-order model (see Table 3 and the Supporting Information, Figure S5), the pseudo-second-order model is better to describe the adsorption kinetics of MO on PANI/α-ZrP and PANI nanotubes.

4. CONCLUSIONS

In this study, novel organic−inorganic hybrid material of polyaniline/α-zirconium phosphate nanocomposites were synthesized by in situ oxidative polymerization and MO adsorption onto the hybrid materials was investigated. Characterized results showed that PANI was successfully grafted on the surface of α-ZrP. The maximum adsorption capacity of PANI/α-ZrP toward MO was 377.5 mg g^{-1}, which is much higher than that of many other adsorbents. The mechanical and chemically stable inorganic α-ZrP can be a good substrate for the growth of smaller and uniformly

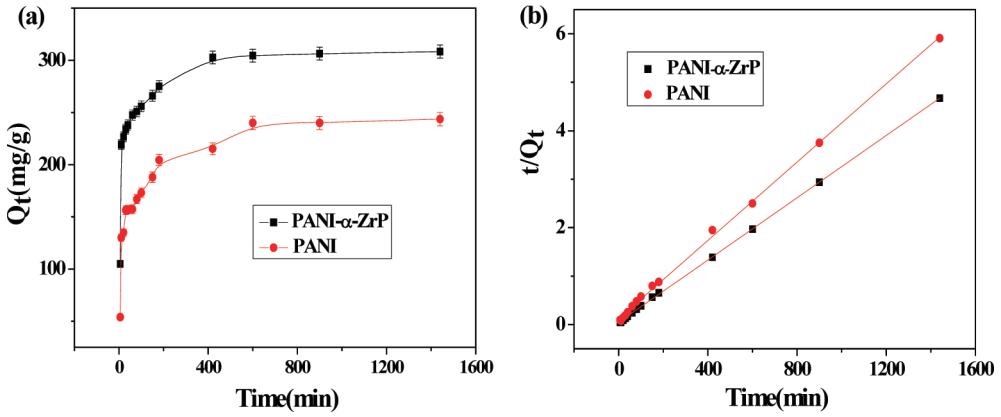

Figure 6. (a) Adsorption kinetics curves and (b) pseudo-second-order kinetic plots for the adsorption of MO with initial concentration of 100.0 mg L^{-1} by PANI nanotubes and PANI/α-ZrP nanocomposites.

Table 3. Kinetics Parameters for the Adsorption of MO on PANI Nanotubes and PANI/α-ZrP Nanocomposites

		first-order kinetics			second-order kinetics		
adsorbent	q_{exp} (mg/g)	k_1(1/min)	q_{cal}(mg/g)	R^2	k_2(g/(mg·min))	q_{cal}(mg/g)	R^2
α-ZrP/PANI	308	3.5×10^{-3}	66.5	0.966	2.8×10^{-4}	310	0.999
PANI	243	4.1×10^{-3}	104.0	0.966	1.5×10^{-4}	247	0.999

dispersed PANI fibrillar nanostructure on the α-ZrP surface, providing more active binding sites for MO. Thus, a synergistic effect of PANI and α-ZrP on promoting the adsorption removal of MO was found. MO adsorption isotherms on PANI/α-ZrP can be well-fitted by the Langmuir model, indicating of a monolayer adsorption, and the adsorption kinetics follows the pseudo-second-order model. The experimental results imply that the hybrid material of PANI/α-ZrP might be a potential candidate for the removal of organic pollutants from large volumes of aqueous solutions.

■ ASSOCIATED CONTENT

Supporting Information

Calibration curve of MO solutions; UV−vis spectra of MO adsorption on α-ZrP as the function of solution pH; UV−vis spectra of MO adsorption on α-ZrP, PANI, and PANI/α-ZrP(α-ZrP/aniline mol ratio = 1:5, 1:10, 1:15, 1:20, 1:30, and 1:40) samples; Freundlich isotherm model plots of MO on PANI nanotubes and on PANI/α-ZrP nanocomposites; pseudo-first-order kinetics plots of MO on PANI nanotubes and on PANI/α-ZrP nanocomposites; effect of pH on the removal of CR and MB by PANI/α-ZrP nanocomposites; adsorption isotherm of CR and MB on PANI/α-ZrP nanocomposites. This material is available free of charge via the Internet at http://pubs.acs.org.

■ AUTHOR INFORMATION

Corresponding Author

*E-mail: anwuxu@ustc.edu.cn (A.-W.X.); whxu@iim.ac.cn (W.-H.X). Phone: (86) 551-3602346. Fax: (86)-551-3600246.

Author Contributions

‖These two authors contributed equally to this work

Notes

The authors declare no competing financial interest.

■ ACKNOWLEDGMENTS

This research was supported by the National Basic Research Program of China (2011CB933700, 2010CB934700), the One Hundred Person Project of the Chinese Academy of Sciences, and the Natural Science Foundation of China (20971118, 50901073).

■ REFERENCES

(1) Ayad, M. M.; Abu El-Nasr, A. *J. Phys. Chem. C* **2010**, *114*, 14377.
(2) Gong, J. L.; Wang, B.; Zeng, G. M.; Yang, C. P.; Niu, C. G.; Niu, Q. Y.; Zhou, W. J.; Liang, Y. *J. Hazard. Mater.* **2009**, *164*, 1517.
(3) Lee, C. K.; Wang, C. C.; Juang, L. C.; Hsu, T. C.; Lee, J. F.; Huang, F. C. *J. Colloid Interface Sci.* **2004**, *273*, 80.
(4) Dogan, M.; Karaoglu, M. H.; Alkan, M. *Microporous Mesoporous Mater.* **2009**, *122*, 20.
(5) Mckay, G.; Ramprasad, G.; Mowli, P. P. *Water Air Soil Pollut.* **1986**, *29*, 273.
(6) Singh, K. P.; Mohan, D.; Sinha, S.; Tondon, G. S.; Gosh, D. *Ind. Eng. Chem. Res.* **2003**, *42*, 1965.
(7) Gupta, V. K.; Suhas; Ali, I.; Saini, V. K. *Ind. Eng. Chem. Res.* **2004**, *43*, 1740.
(8) Mittal, A.; Kurup, L.; Gupta, V. K. *J. Hazard. Mater.* **2005**, *117*, 171.
(9) Chatterjee, D.; Patnam, V. R.; Sikdar, A.; Moulik, S. K. *J. Chem. Eng. Data* **2010**, *55*, 5653.
(10) Walcarius, A.; Mercier, L. *J. Mater. Chem.* **2010**, *20*, 4478.
(11) Paul, M.; Pal, N.; Rajamohanan, P. R.; Rana, B. S.; Sinha, A. K.; Bhaumik, A. *Phys. Chem. Chem. Phys.* **2010**, *12*, 9389.
(12) Swain, S. K.; Mishra, S.; Sharma, P.; Patnaik, T.; Singh, V. K.; Jha, U.; Patel, R. K.; Dey, R. K. *Ind. Eng. Chem. Res.* **2010**, *49*, 9846.
(13) Jin, X. L.; Yu, C.; Li, Y. F.; Qi, Y. X.; Yang, L. Q.; Zhao, G. H.; Hu, H. Y. *J. Hazard. Mater.* **2011**, *186*, 1672.
(14) Lin, Y. X.; Cai, W. P.; Tian, X. Y.; Liu, X. L.; Wang, G. Z.; Liang, C. H. *J. Mater. Chem.* **2011**, *21*, 991.
(15) Zhai, J. P.; Zhang, Y.; Li, Q.; Sun, L.; Tang, R. *J. Hazard. Mater.* **2010**, *175*, 404.
(16) Pan, B.; Zhang, Q.; Du, W.; Zhang, W.; Pan, B.; Zhang, Q.; Xu, Z.; Zhang, Q. *Water Res.* **2007**, *41*, 3103.
(17) Pei, Q. B.; Yu, G.; Zhang, C.; Yang, Y.; Heeger, A. J. *Science* **1995**, *269*, 1086.
(18) MacDiarmid, A. G. *Angew. Chem., Int Ed.* **2001**, *40*, 2581.

(19) Jiang, J. Z.; Liu, J. F.; Yin, S.; Wu, H. P.; Zeng, Y. W.; Hu, X. R.; Wang, Y. W.; Lv, G. L. *J. Phys. Chem. B* **2006**, *110*, 21588.
(20) Sanchez, C.; Julian, B.; Belleville, P.; Popall, M. *J. Mater. Chem.* **2005**, *15*, 3559.
(21) Sue, H. J.; Sun, L. Y.; Boo, W. J.; Clearfield, A. *New J. Chem.* **2007**, *31*, 39.
(22) Sue, H. J.; Gam, K. T.; Bestaoui, N.; Spurr, N.; Clearfield, A. *Chem. Mater.* **2004**, *16*, 242.
(23) De, S.; De, A.; Das, A. *Mater. Chem. Phys.* **2005**, *91*, 477.
(24) Takei, T.; Kobayashi, Y.; Hata, H.; Yonesaki, Y.; Kumada, N.; Kinomura, N.; Mallouk, T. E. *J. Am. Chem. Soc.* **2006**, *128*, 16634.
(25) Furukawa, Y.; Ueda, F.; Hyodo, Y.; Harada, I.; Nakajima, T.; Kawagoe, T. *Macromolecules* **1988**, *21*, 1297.
(26) Wu, X. L.; Zhao, D. L.; Yang, S. T. *Desalination* **2010**, *269*, 84.
(27) Langmuir, I. *J. Am. Chem. Soc.* **1918**, *40*, 1361.
(28) Freundlich, H. M. F. *J. Phys. Electrochem.* **1906**, *57*, 385.
(29) Chowdhury, A. N.; Jesmeen, S. R.; Hossain, M. M. *Polym. Adv. Technol.* **2004**, *15*, 633.
(30) Gezici, O.; Ayar, A.; Kucukosmanoglu, M. *J. Hazard. Mater.* **2007**, *146*, 186.
(31) Juang, R. S.; Annadurai, G.; Lee, D. J. *J. Hazard. Mater.* **2002**, *92*, 263.
(32) Huang, J. H.; Huang, K. L.; Liu, S. Q.; Wang, A. T.; Yan, C. *Colloids Surf. A* **2008**, *330*, 55.
(33) Ni, Z. M.; Xia, S. J.; Wang, L. G.; Xing, F. F.; Pan, G. X. *J. Colloid Interface Sci.* **2007**, *316*, 284.
(34) Jalil, A. A.; Triwahyono, S.; Adam, S. H.; Rahim, N. D.; Aziz, M. A. A.; Hairom, N. H. H.; Razali, N. A. M.; Abidin, M. A. Z.; Mohamadiah, M. K. A. *J. Hazard. Mater.* **2010**, *181*, 755.
(35) Ma, J.; Qin, Q. D.; Liu, K. *J. Hazard. Mater.* **2009**, *162*, 133.
(36) Ai, L. H.; Jiang, J.; Zhang, R. *Synth. Met.* **2010**, *160*, 762.
(37) McKay, G.; Ho, Y. S. *Process Biochem.* **1999**, *34*, 451.